Conf-950216--76
SAN095-0271C

A NATURAL ANALOGUE FOR HIGH-LEVEL WASTE IN TUFF: CHEMICAL ANALYSIS AND MODELING OF THE VALLES SITE

H.W. Stockman, J.L. Krumhansl, and C.K. Ho (Sandia National Laboratories, Albuquerque NM); L. Kovach (U.S. Nuclear Regulatory Commission, Washington DC); and V.S. McConnell (University of Alaska, Fairbanks AK).

ABSTRACT

The contact between an obsidian flow and a steep-walled tuff canyon was examined as an analogue for a high-level waste repository. The analogue site is located in the Valles Caldera in New Mexico, where a massive obsidian flow filled a paleocanyon in the Battleship Rock Tuff. The obsidian flow provided a heat source, analogous to waste panels or an igneous intrusion in a repository, and caused evaporation and migration of water. The tuff and obsidian samples were analyzed for major and trace elements and mineralogy by INAA, XRF, X-ray diffraction, and scanning electron microscopy and electron microprobe. Samples were also analyzed for D/H and $^{39}Ar/^{40}Ar$ isotopic composition. Overall, the effects of the heating event seem to have been slight and limited to the tuff nearest the contact. There is some evidence of devitrification and migration of volatiles in the tuff within 10 m of the contact, but variations in major and trace element chemistry are small and difficult to distinguish from the natural (pre-heating) variability of the rocks.

INTRODUCTION

The U.S. Department of Energy has selected the Yucca Mountain Site (YMS), located in Nevada, as a potential repository for disposal of high-level commercial radioactive waste. Yucca Mountain is composed of rhyolite tuffs, in various states of welding and devitrification. To determine the suitability of YMS for safe storage, it is necessary to predict the chemical and physical response of the tuffs to local and site-wide heating for 10,000 years. For over a decade, scientists have used geochemical, thermal-hydrologic, and geomechanical codes to model the interaction of the tuffs, groundwater, and the radioactive waste. Most models focus on the degradation of the waste containers, dissolution of radionuclides in the waste, and the eventual diffusion, advection and sorption of the dissolved contaminants [1]. However, the dissolution of the tuff minerals, and consequent reprecipitation in cooler regions, generation of halogen-rich gases, and polymorphic transitions must also be modeled, since these processes affect permeability and structural integrity of the host rocks.

Uncertainty in the models arises from the need to extrapolate from equilibrium conditions, or small-scale experiments performed on the bench top over days or months, to meter- and km-scale processes occurring in the repository over thousands of years. Radionuclide solubility and sorption calculations are based principally on equilibrium thermodynamics, and a limited number of laboratory tests to assess the rate of important reactions. The accuracy of the extrapolations can have a dramatic effect on the predicted safety of the repository. For example, some models predict that clinoptilolite, which strongly absorbs Cs and Sr, will form as the tuffs alter; other models predict the formation of less-sorptive mordenite, or even

This work was supported by the United States Department of Energy under Contract DE-AC04-94AL85000.

TJ

DISCLAIMER

Portions of this document may be illegible in electronic image products. Images are produced from the best available original document.

a non-sorptive feldspar-quartz assemblage from the same rocks [2,3].

One means to reduce this uncertainty is to study natural analogues -- large masses of geologic materials that were subject, over hundreds to millions of years, to processes analogous to those expected for the repository. The Valles Caldera, located in the Jemez Mountains of northern New Mexico (figure 1A), provides a good natural analogue for many of the processes expected at YMS. In the southeast corner of the caldera, the Banco Bonito obsidian (BBO) flow filled a steep-walled canyon cut in the Battleship Rock tuff (BRT). The obsidian, initially at temperatures in excess of 850°C , heated the porous tuff in the canyon walls and vaporized much of the pore water. The goals of the Valles Natural Analogue Project were to: (1) search for evidence of chemical and mineralogic changes in the tuff -- specifically changes that occurred in response to the heating event; (2) provide a well-characterized example for testing chemical migration models; and (3) provide guidance for future analogue studies and code development.

{PLACE FIG. 1 HERE}

GEOLOGICAL BACKGROUND

The Valles Caldera formed following the eruption of the Otowi and Tshirege Members of the Bandelier Tuff, at 1.45 and 1.1 Ma [4]. Subsequent to the last major eruption of the Bandelier tuff, the caldera collapsed and a lake formed in the central depression. The Deer Canyon Rhyolite erupted in the central portion of the caldera, accompanied by landslides off the topographic rim, so that approximately 600 m of fill was deposited over the foundered cauldron floor. As lacustrine deposition waned, a resurgent dome (Redondo Peak) with $\approx$900 m of relief formed in the central portion of the caldera. From the beginning of resurgence to 540 kA, numerous rhyolite dome erupted along the ring fracture. The last volcanic activity in the region included eruption of the BRT. A deep, steep-walled canyon was eroded into the tuff, and the canyon was subsequently filled by the BBO flow. The ages of these units are uncertain because of ambiguities inherent in current dating methods [5]; however, 40Ar/39Ar ages obtained for this study show both units are 400 to 250 kA old. After the BBO filled the ancestral canyon, the modern-day San Diego Canyon was eroded to the west, exposing much of the BRT-BBO contact. For the purposes of this study, the BRT is analogous to the tuffs at the YMS, and the BBO provides a heat source analogous to repository waste panels or a disruptive igneous intrusion, and the contact region between the two units is the focus of our analyses.

SAMPLING AND METHODS

Initial samples were taken from VC-1, a vertical core hole drilled through a lobe of the BBO. However, the VC-1 samples suffered several limitations. First of all, the core samples are small and potentially unrepresentative. More important, the BRT-BBO contact in the corehole is represented by a thick breccia zone, smearing and adding ambiguity to any observed chemical trends. Therefore samples were obtained from the cliffs of the present-day San Diego Canyon, where the BRT-BBO contact is exposed in outcrop (figures 1B and 1C). These outcrops are near the very edge of the flow, where the flow stopped against the steep walls of the ancestral canyon;

consequently the breccia zone is small to non-existent. Samples were taken from "horizontal" contacts (figure 1C), which provided long sampling paths, and vertical contacts (figure 1B) where there is little possibility of contamination by a soil layer.

Bulk chemical and mineral analyses were obtained by a variety of techniques, including: instrumental neutron activation analysis (INAA), for trace elements such as U, Th, Cs, Rb, Ba, Ta, Hf and rare earths; glass disc X-ray fluorescence (XRF) for major elements; pressed-pellet XRF for Cl and S; ion chromatography (IC) for leachable anions; fluoride ion-specific electrodes; and X-ray diffraction (XRD), electron microprobe (EMP), and scanning electron microscopy (SEM) to identify and analyze mineral phases and the abundance of glass. To test effects of heterogeneity, the tuffs were broken down into fine-grained matrix components and clasts (including xenoliths from older units), and heavy mineral separates. Differences between matrix and whole rock analyses proved to be small, and it was determined that the abundance of heavy minerals (including oxides and sphene, as well as micas, pyroxenes and amphiboles) was too small to account for significant variations in rare earth, F, and U or Th contents.

RESULTS

Figure 2 gives a sample of chemical variations observed at two outcrop sites as a function of distance from the BRT-BBO contact. In short, most non-volatile trace elements showed very little variation. Variations of most other analytes were quite small; for example, bulk silica in the site 13 tuffs varied from ca. 70% to 72%, with standard deviation less than 1%. Figures 2A and 2B show representative volatile contents at site 12, a vertical contact, and site 13, a "horizontal" contact (the latter has a horizontal exposure, but the BRT-BBO interface dips into the cliff face at ≈45°). Note the large difference in the distance scale for the two sites. In all sites examined, F and Cl have an antipathetic behavior, with Cl depleted near the contact, and F enriched in the same region. Physical effects of the heating are more pronounced at site 12, where the tuff nearest the contact is deformed and obsidian clasts are oriented parallel to the contact; evidently, the contact tuffs were raised above the glass point (ca. 670°C). At site 13, the tuffs nearest the contact have lower glass contents (are more devitrified), and are depleted in Cl and water; there is also a slight but statistically significant increase in δD near the contact. In contrast, non-volatile trace elements such as Ce, U and Ta (figures 2C and 2D) show little or no systematic variation. Cs may increase slightly toward the contact, but the increase corresponds to systematic changes in CaO, FeO and Na_2O contents, and may reflect original variations in tuff composition.

{PLACE FIG 2 HERE}

Mineralogical changes in the tuffs, as a consequence of heating, are slight. The voids of pumice shards that comprise the tuff matrix are lined with delicate, sub-μm-sized lathes of albite and less abundant silica polymorphs; qualitatively, the amount of void-lining drops off with distance from the contact. Near the contacts, the matrix glass shards have partly devitrified to micro-porous, extremely fine-grained intergrowths of feldspar and silica. The Rb/Cs, a potentially sensitive indicator for clay/zeolite development, shows little variation (figure 2C). Neither XRD nor SEM analyses showed unambiguous development of zeolites or clays in the outcrop samples. Attempts to beneficiate fine-grained zeolites and clays, by standard settling techniques,

yielded no clay or zeolite peaks in XRD spectra.

GAS TRANSPORT EXPERIMENTS

The chemical analyses above suggest we should seek mechanisms for transport and concentration of volatiles, particularly F, Cl and water. We developed a simple thermal for the obsidian flow-tuff system, based on the Stefan solution [6,7], that accounted for evaporation, convection and radiation at the top of the obsidian flow, and boiling and conduction at the BRT-BBO contact. Because the tuff is very porous and has a comparatively low conductivity, temperatures well above the glass point could be sustained at the contact for hundreds of years, consistent with our observations of plastic deformation in the vertical contacts. In addition, the boiling front may have been tens of m from the contact for up to a thousand years. Thus it is important to examine the behavior of the halides in steam, and determine if gaseous transport, alone or in concert with some other mechanism, could lead to the observed variations in F and Cl abundances (figure 2).

A simple flow-through system was constructed to measure realease rates of F, Cl and metals from tuff as a function of temperature and time. Sample of crushed, washed tuff were packed between wads of silica wool in a 2.5 cm diameter, 50 cm long silica tube, and the tube was placed in a tube furnace. By means of a silica carburetor and low-volume peristaltic pump, steam was fed through the system, condensed, and collected for INAA and IC analysis (apart from Na, no trace elements were detected by INAA). Two experiments were performed; in the first, the temperature was ramped from 125 to 800 °C, and held at each increment for several hours; 1383 g of steam was passed through 33.2 g of tuff in 15 days. In the second, the sample was held at 400 °C for 54 hours; 172 g of steam was passed through 33.8 g of tuff.

Results of the two experiments are shown in figures 3A and 3B. Figure 3A gives the apparent gas/rock K_D. While there is divergent behavior of Cl and F at $T < 600$ °C, the apparent K_D is «1 for both elements in this range, suggesting that steam-rock partitioning alone is a poor mechanism for causing the antipathetic behavior of Cl and F (figure 2A), and is probably inadequate to explain the F concentrations observed near the BRT-BBO contacts. However, the interaction can produce steam containing tens of ppm F, which may condense and interact with tuff elsewhere. Figure 2B, for the second experiment, shows the decrease in loss rate with time. The fitted curves assume a pure diffusion model for release of F and Cl from the glass shards, assuming the glass septa are ≈10 μm thick (consistent with SEM examination). The regression line for F yields an initial matrix F of ≈ 277 ppm, consistent with our chemical analyses, and a diffusion coefficient of $1.5 \cdot 10^{-12}$ cm^2/sec. The solid line fitted to the Cl data uses all points; the dashed line omits the first 3, which are potentially contaminated with the system blank. These two fits yield initial Cl of 2.7 and 4.2 ppm respectively, and diffusion coefficients of $6.3 \cdot 10^{-12}$ and $1.6 \cdot 10^{-12}$. The calculated initial Cl contents are clearly wrong, suggesting the control on Cl loss is not pure diffusion. However, the calculated 400 °C diffusion coefficients for both F and Cl are consistent with literature estimates [8,9].

{PLACE FIG. 3 HERE}

CHEMICAL VARIATIONS INDUCED BY CAPILLARITY/EVAPORATION

The existence of a boiling front can create complex compositional variations in heated tuffs. Travis and Nuttall [10] calculated the distribution of SiO_2 and Cl in fractured and porous tuff, as functions of time and distance from the waste canister heat source. A hot, dry zone forms immediately around the canister; the boiled water condenses several m away, yielding a concentric zone of saturation. Capillary action draws the water outward from the condensation zone; not only is the water drawn away from the heat source, out into the cooler tuff, but it is also drawn back towards the heat source. At a given time, whole rock SiO_2 and Cl tend to peak on both sides of the condensation zone. On the hot side, evaporation tends to concentrate the solutions and cause SiO_2 precipitation, whereas in the cool region, the inherent decrease in SiO_2 solubility with decreasing temperature also causes a SiO_2 buildup. These calculations suggest one should search for regions of silica and halide enrichment as proof of the capillarity/evaporation model, yet are inconsistent with the lack of significant trends in bulk silica content at the Valles analogue. However, Travis and Nutall did not consider the dissolution of other silicates, nor the possibility that the silicate deposition would be lost in the larger matrix variations.

A simple, heuristic model was developed to predict mineralogical and bulk F and silica variations in the boiling region. From SEM examination of the relative volumes of voids, pumice solids, and the crystalline void fillings, we estimate an effective water/rock volume ratio ranging from 100/3.5 to 100/30 for 50% to 100% saturation. The walls of the voids and the fine-grained ($\approx$0.3 μm width), high-surface-area crystallites lining the voids are assumed to be the most chemically active part of the system, and the denser clasts and glass shards (which show little sign of alteration) are assumed to be inert. We assume there is a relatively large, wet source region where water equilibrates with tuff at $\approx$100 °C, and this water is subsequently pulled into the boiling region by capillarity, where minerals precipitate, existing minerals are altered by interaction with the solution, and the aqueous phase becomes enriched in components such as Na and F. The calculations were run with the *react* code, assuming atmospheric O_2 and CO_2 fugacities. In some runs precipitation of all silica polymorphs except chalcedony was suppressed to allow clinoptilolite to form, which has a dramatic effect on the sorption of Cs but very little effect on the major element chemistry of the bulk precipitates.

Figure 4A shows how the void mineralogy changes for a sample calculation, expressed as g of solids per kg of water. The relative amounts of major silicates change little, especially after about 30 pore volumes have evaporated. However, the F content of the precipitates increases steadily as fluorite precipitates. The predicted change in the bulk rock chemistry (including contributions form the inert matrix) is +0.1% for silica, and +867 ppm F after about 60 pore volumes are evaporated. The change in silica is completely insignificant compared to the ±0.6% variation observed for pairs of adjacent samples taken far from the contact. However, the change in F content is several times the native F content of the tuffs, and is consistent with the F enrichment levels seen at site 12 (figure 2A).

{PLACE FIG. 4 HERE}

Figure 4B illustrates that complex trace element variations can arise from this simple model. Translated into bulk rock concentrations, the precipitation of $Na_2U_2O_7$ could elevate the bulk U

content by ≈10 ppm in the intermediate stages of evaporation. However, as the system becomes more alkaline with increased evaporation, the U solids redissolve.

CONCLUSIONS

The BRT shows remarkably little alteration from the heating event. There is some evidence for devitrification, loss of volatiles, precipitation of albite-silica in voids, and perhaps redistribution of fluorine within 10 m of the contact. There has been little development of sorptive phases such as zeolites and clays, and there is no evidence for extensive silica remobilization in the bulk analyses. These results are consistent with a simple model for concentration of solutes and precipitation of minerals in the boiling zone.

REFERENCES

1. Pigford, T.H.; Chambré, P.L. and Lee, W. W.-L. (1992) A review of near-field mass transfer in geologic disposal systems, *Radioactive Waste Management and the Nuclear Fuel Cycle*, v **16**, pp 175-276.

2. Criscenti, L.J. and Arthur, R.C. (1991) The calculated effects of isothermal boiling on tuff-water interactions, *Radiochimica Acta* v **52**, pp 513-517.

3. Arthur, R.C. and Criscenti, L.J. (1991) Error evaluation in reactive-solute transport calculations, *Radiochimica Acta* v **52**, pp 507-512.

4. Bailey, R.A.; Smith, R.L. and Ross, C.S. (1969) Stratigraphic nomenclature of volcanic rocks in the Jemez Mountains, New Mexico, *U.S. Geol Surv. Bull.* v **1274-P**, pp 1-19.

5. Self, S.; Wolff, J.A.; Spell, T.L.; Skuba, C.E. and Morrissey, M.M. (1991) Revisions to the stratigraphy and volcanology of the post-0.5 Ma units and the volcanic section of the VC-1 core hole, Valles Caldera, New Mexico, *Jour. Geophysical Research* v **96**, pp 4107-4116.

6. Stockman, H.; Krumhansl, J.; Ho, C. and McConnell, V. *The Valles Natural Analogue Project,* NUREG/CR-6221 (1994).

7. Crank, J. (1984) *Free and Moving Boundary Problems.* Clarendon Press, Oxford, 425 pp.

8. Dingwell, D.B. and Scarfe, C.M. (1985) Chemical diffusion of fluorine in melts in the system Na_2O-Al_2O_3-SiO_2, *Earth and Planetary Science Letters* v **73**, pp 377-384.

9. Jambon, A. (1982) Tracer diffusion in granitic melts: experimental results for Na, K, Rb, Cs, Ca, Sr Ba, Ce, Eu to 1300°C and a model of calculation, *Jour. Geophysical Research* v **87**, pp 10797-10810.

10. Travis, B.J. and Nuttall, H.E. (1987) *Two-Dimensional Numerical Simulation of Geochemical Transport in Yucca Mountain.* LA-10532-MS, Los Alamos National Laboratory, Los Alamos NM 87545.

1A

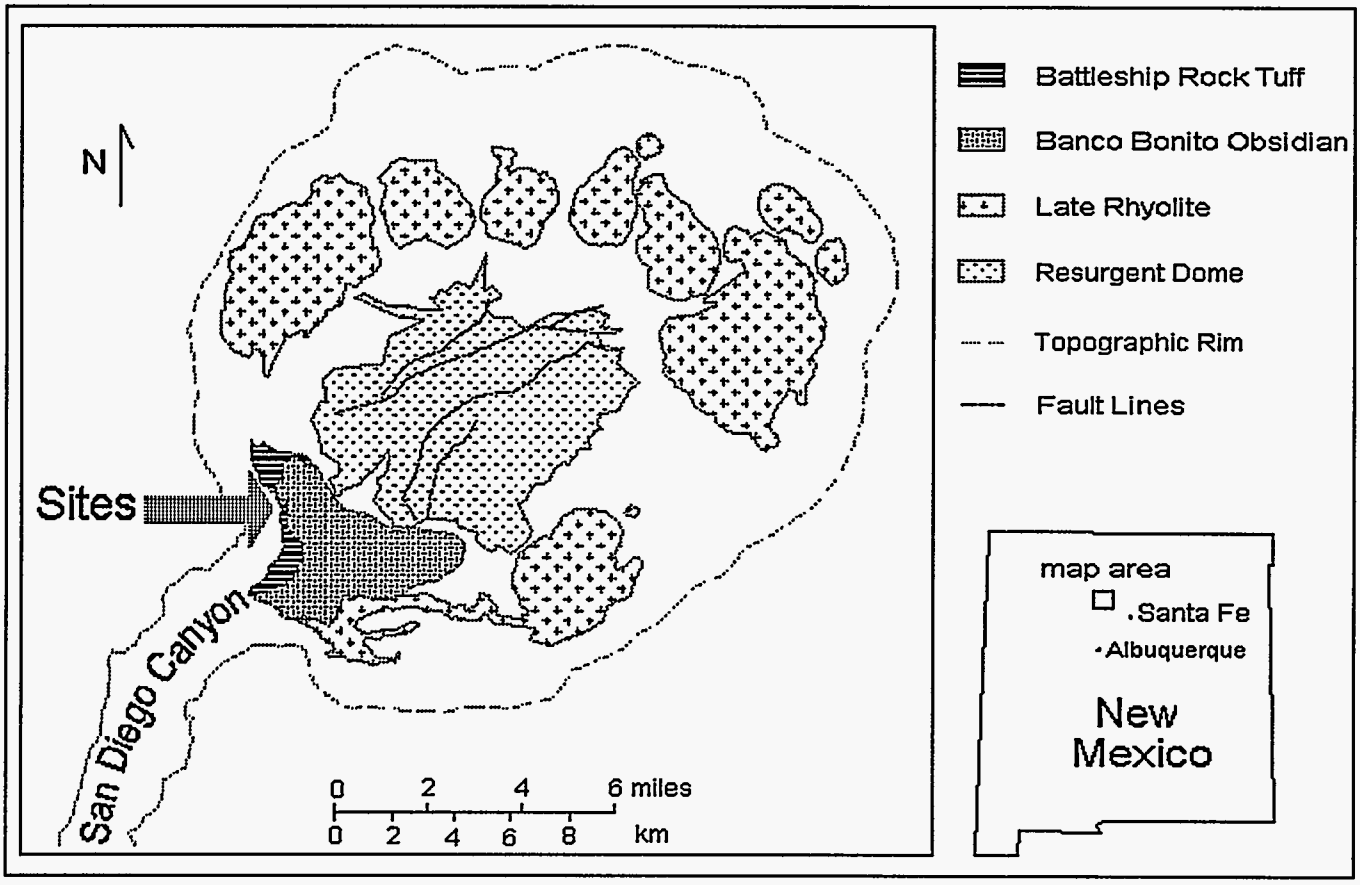
N
Sites
San Diego Canyon
0 2 4 6 miles
0 2 4 6 8 km
Battleship Rock Tuff
Banco Bonito Obsidian
Late Rhyolite
Resurgent Dome
Topographic Rim
Fault Lines
map area
Santa Fe
Albuquerque
New Mexico

1B

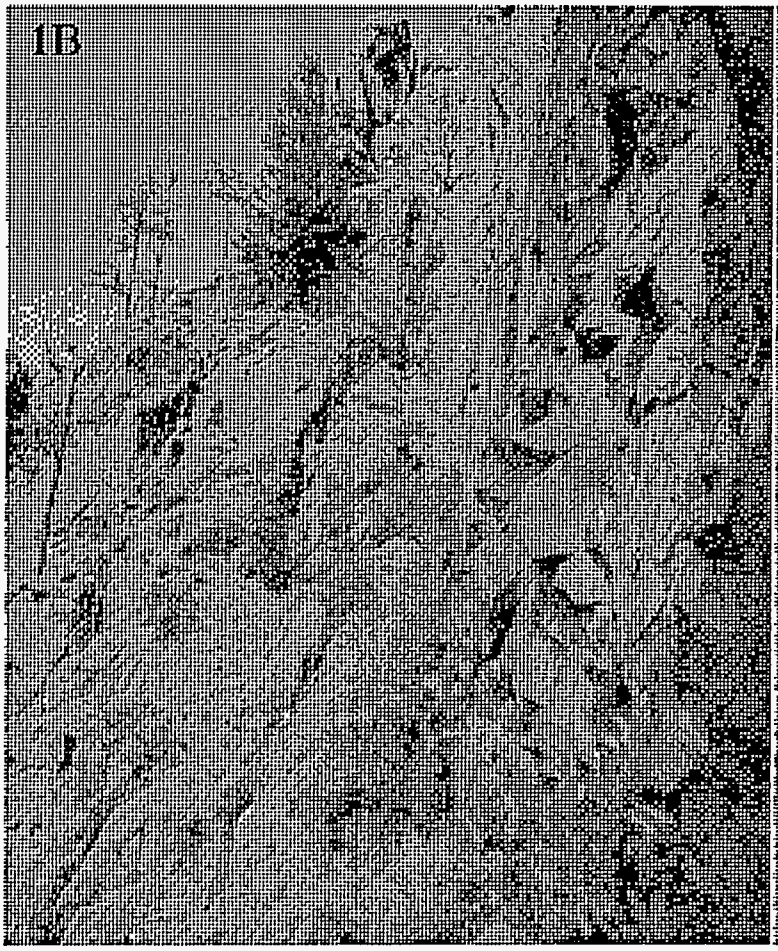

1C

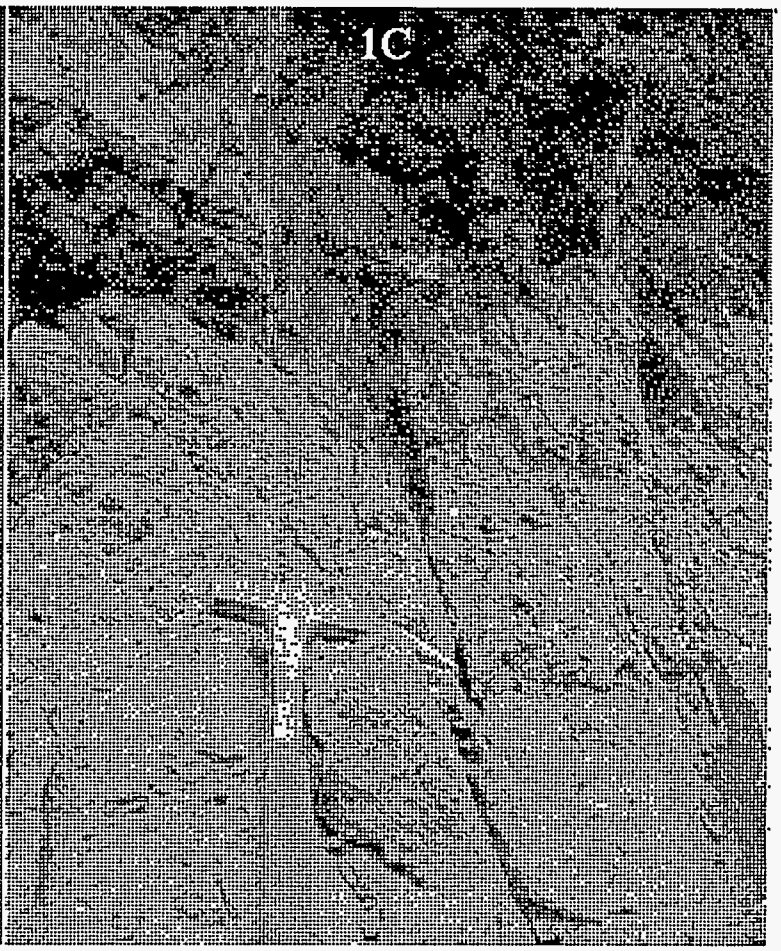

2A (site 12)

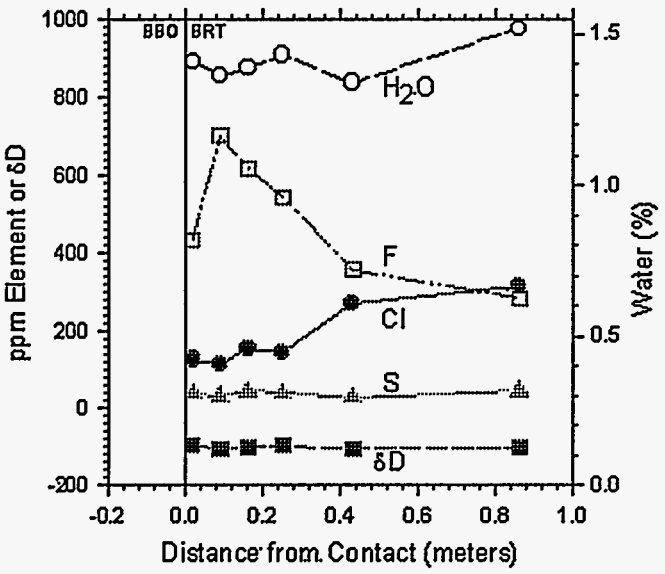

2B (site 13)

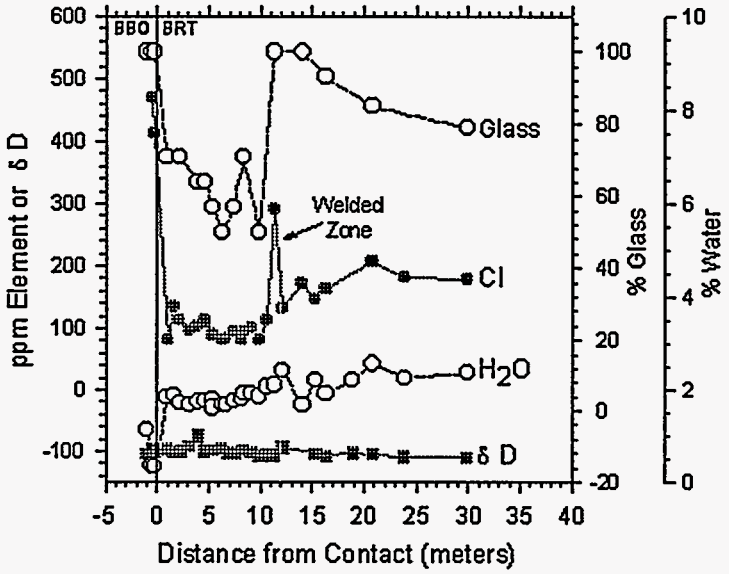

2C (Site 13 and Site 12)

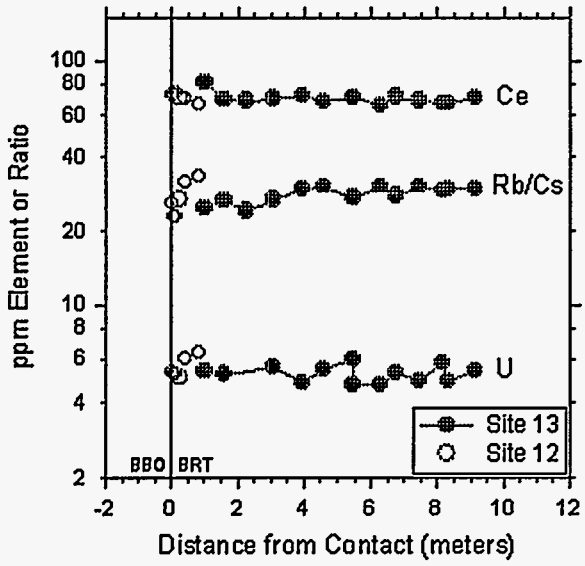

2D (Site 13 and Site 12)

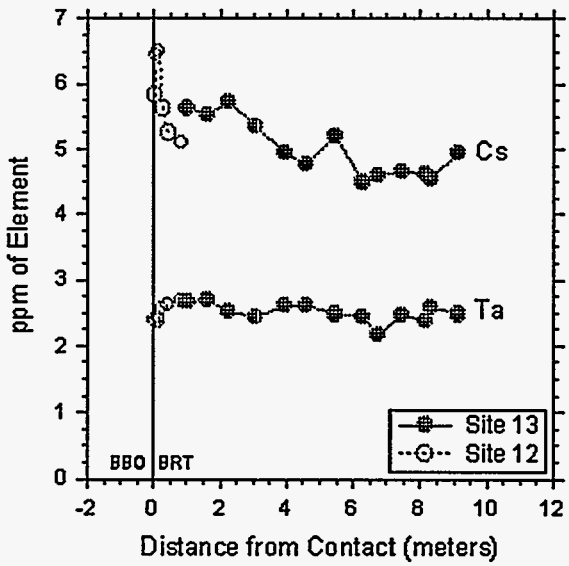

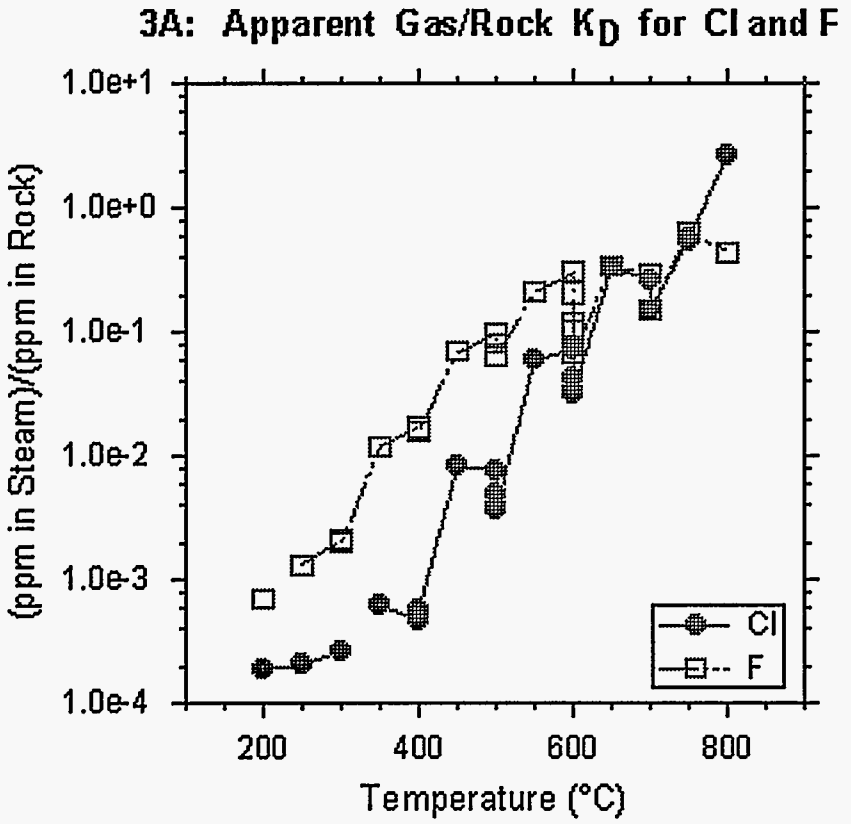
3A: Apparent Gas/Rock K_D for Cl and F
1.0e+1
1.0e+0
1.0e-1
1.0e-2
1.0e-3
1.0e-4
(ppm in Steam)/(ppm in Rock)
200
400
600
800
Temperature (°C)
Cl
F

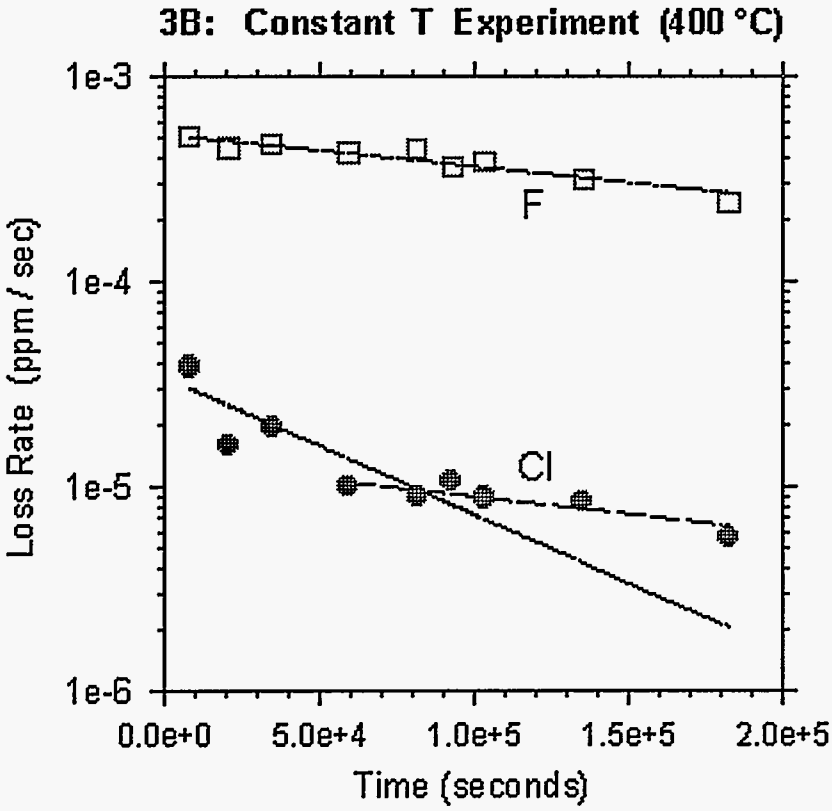
3B: Constant T Experiment (400 °C)
1e-3
1e-4
1e-5
1e-6
Loss Rate (ppm / sec)
0.0e+0
5.0e+4
1.0e+5
1.5e+5
2.0e+5
Time (seconds)
F
Cl

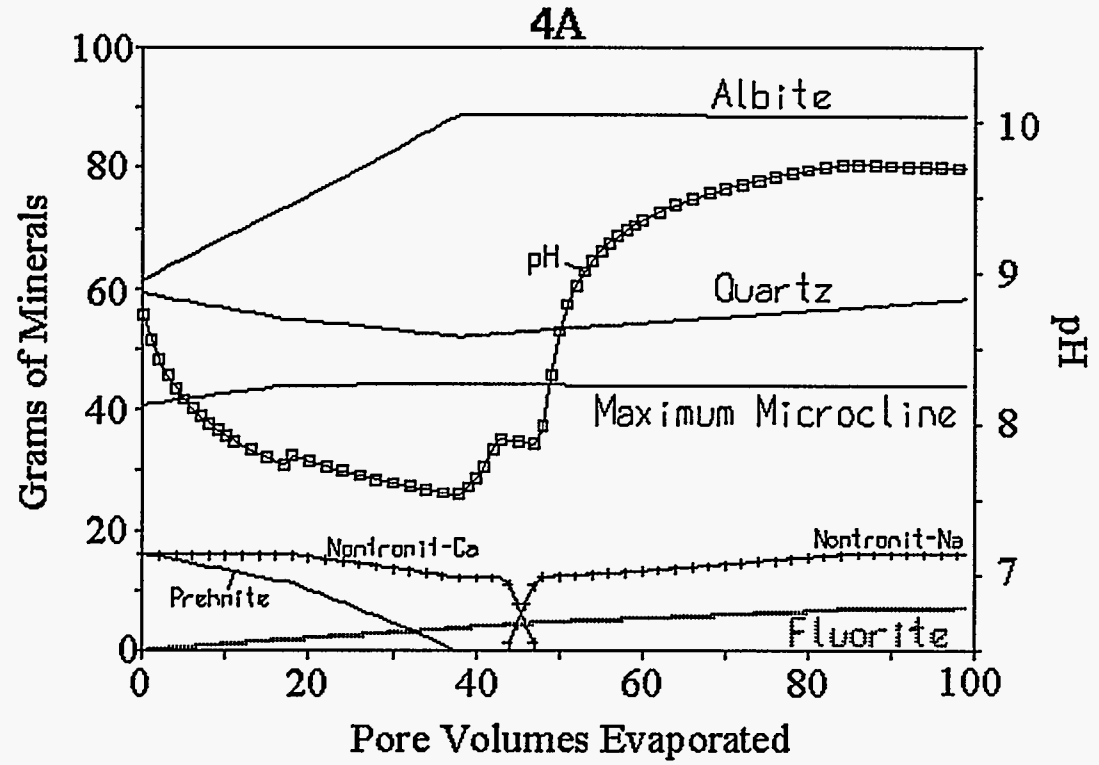

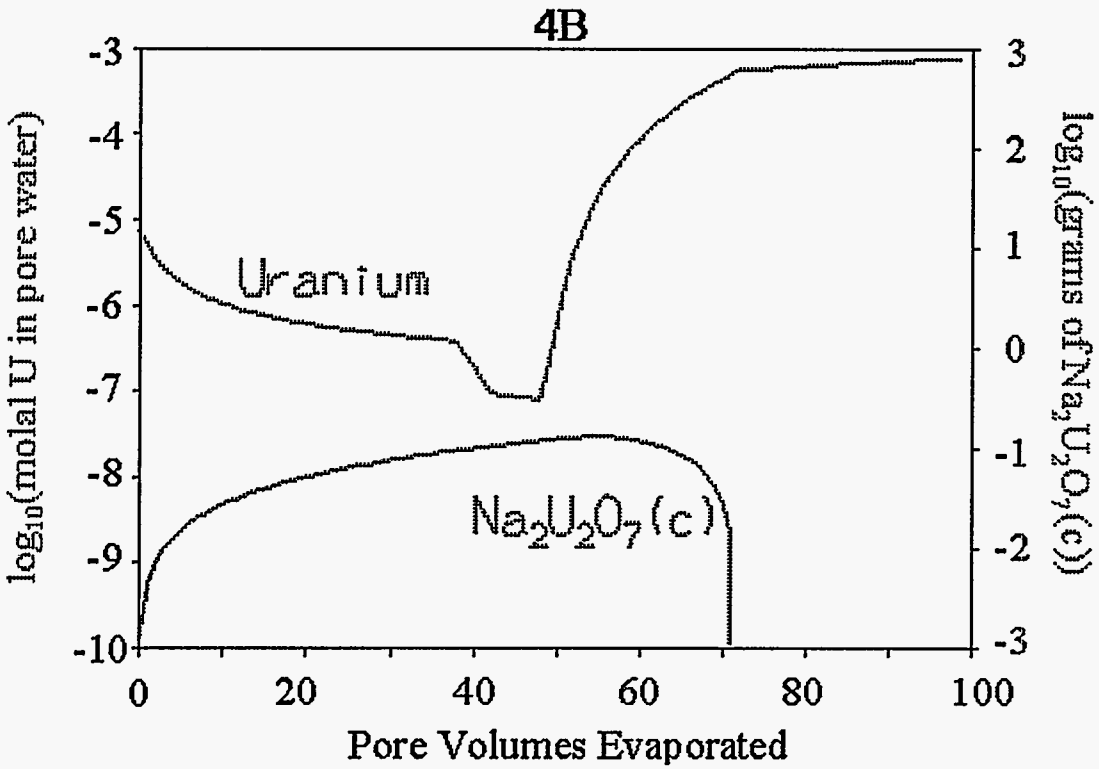

DISCLAIMER